

Decay of a Three-Quasiparticle State in $^{177}\text{Ta}^\dagger$

H. Hübel,* R. A. Naumann, and E. H. Spejewski

*Joseph Henry Laboratories of Physics and Frick Chemical Laboratory,
Princeton University, Princeton, New Jersey 08540*

(Received 28 June 1971)

The decay of a three-quasiparticle isomeric state at 1355 keV in ^{177}Ta was studied using in-beam γ -ray spectroscopic techniques. Tantalum isotopes were produced by the $^{175,176}\text{Lu}(\alpha, xn)$ reactions with α -particle energies between 24 and 48 MeV. The half-life of the isomer was measured to be $t_{1/2}(1355 \text{ keV}) = 5.02 \pm 0.20 \mu\text{sec}$, and its spin and parity were determined to be $I^\pi = \frac{21}{2}^-$. The $E2/M1$ mixing ratios and the rotational-model parameters $(g_K - g_R)^2/Q_0^2$ were deduced for five $\Delta I = 1$ transitions between members of the rotational band based on the $\frac{3}{2}[514]$ state.

I. INTRODUCTION

In (particle, xn) nuclear reactions the angular momentum transferred into the product is quite high. Therefore, high-spin members of collective sequences based on the ground state as well as particle states with large angular momentum can be populated.^{1,2} In many cases the latter include one- or three-quasiparticle states in odd-mass nuclides and two- or four-quasiparticle states in even-mass nuclides which have quite long lifetimes.³⁻⁸

In the region of deformed nuclei the transitions depopulating the isomeric states are often retarded by the K -selection rule.⁹ For the nuclides around $N=106$ and $Z=72$ the Nilsson model^{9,10} predicts a sequence of single-neutron and single-proton states with high K quantum numbers. These are the neutron orbitals with Nilsson configurations $\frac{5}{2}[512]$, $\frac{7}{2}[514]$, and $\frac{9}{2}[624]$, and the proton orbitals with $\frac{7}{2}[404]$, $\frac{9}{2}[514]$, and $\frac{5}{2}[402]$. High-spin one-, two-, three-, and four-quasiparticle excitations involving these states in various combinations have been experimentally found to exist.^{3-8, 11, 12}

Recently, some investigations of the level schemes of ^{175}Ta and ^{177}Ta using $^{175}\text{Lu}(\alpha, xn)^{179-x}\text{Ta}$ reactions have been reported.¹³⁻¹⁷ Rotational sequences based on single-particle states with Nilsson quantum numbers $\frac{7}{2}[404]$, $\frac{5}{2}[402]$, $\frac{9}{2}[514]$, and $\frac{1}{2}[541]$ have been populated in these reactions up to high-spin values. Furthermore, Geiger, Graham, and Ward (GGW)¹⁴ and Skånberg, Hjorth, and Ryde (SHR)¹⁶ give evidence for a high-spin isomeric state in ^{177}Ta . The excitation energy of the isomer was found to be¹⁶ 1355 keV, and for the half-life the limits $200 \text{ nsec} \leq T_{1/2} \leq 30 \mu\text{sec}$ were given.¹⁶ GGW¹⁴ tentatively assign spin and parity $I^\pi = \frac{21}{2}^-$ to this state. This assignment is also favored by the results of SHR,¹⁶ but $I^\pi = \frac{19}{2}^+$ and $I^\pi = \frac{23}{2}^-$ cannot be excluded.

In this work we report investigations of the γ -ray spectra associated with $^{175}\text{Lu}(\alpha, xn)$ and $^{176}\text{Lu}(\alpha, xn)$ reactions at several α -particle energies. It was the main purpose of these investigations to determine the half-life, spin, and parity of the 1355-keV isomeric state in ^{177}Ta . The properties of the rotational band built on the $\frac{9}{2}[514]$ proton state at 74 keV in ^{177}Ta , which is populated through the $I = \frac{19}{2}$ member by the decay of the isomer, are redetermined and discussed. The decay scheme of one- and three-quasiparticle states in ^{177}Ta , incorporating the results of this work as well as previous investigations,¹³⁻¹⁷ is shown in Fig. 1.

II. EXPERIMENTAL PROCEDURE

The studies of γ rays following $^{176,175}\text{Lu}(\alpha, xn)$ reactions was performed at the Princeton variable-

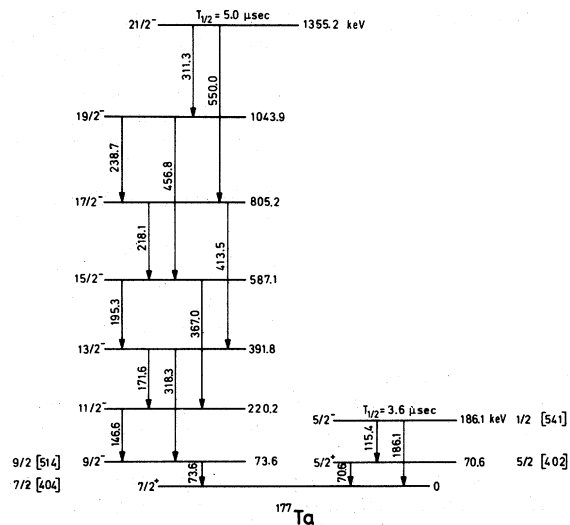


FIG. 1. Decay of one- and three-quasiparticle states in ^{177}Ta .

energy sector-focusing cyclotron.¹⁸ A floor plan indicating the experimental arrangement of the laboratory is shown in Fig. 2.

The Faraday cup is located approximately 5.5 m downstream from the target and is heavily shielded with iron and concrete. A pair of slits is located approximately 3.5 m upstream and is well shielded by the concrete wall. To provide extra shielding at the location of the detectors a small lead cave was built around the scattering chamber and the detectors.

The scattering chamber consists of a closed aluminum cylinder. It is approximately 10 cm in diameter and 10 cm in height. On one side of the chamber, a window of 0.5-mm thickness is cut into the aluminum wall to permit almost attenuation-free γ -ray spectroscopy. The rectangular shape of the window allows angular distributions to be measured at angles up to 150° with respect to the beam line.

On the chamber wall opposite this window, a flange which can be used in several ways is provided. Either a Lucite window which allows the beam spot at the target position to be viewed with a television camera, or a thin aluminum window for γ -ray measurements can be mounted. In addition, it is also possible to insert a cooled Si(Li)

spectrometer for conversion-electron spectroscopy.

The target holder is mounted on a rod which is placed in the bottom lid of the chamber, permitting targets to be rotated and adjusted in height externally. For target changes, two gate valves at both ends of the chamber can be closed, air let into the chamber, and the top lid removed.

For γ -ray spectroscopy, a Ge(Li) detector was used having an active volume of 15 cm^3 and a system resolution, in-beam, of approximately 5 keV for the 511-keV line. Only singles γ -ray measurements at an angle of 90° with respect to the beam line were performed in the experiment described here.

γ -ray energy-calibration spectra were taken before and after each individual run using International Atomic Energy Agency (IAEA) standard sources in place of the target. A $^{177\text{m}}\text{Lu}$ source and IAEA standard sources served as a basis for the Ge(Li) detector efficiency calibration.

Targets were prepared from oxides of ^{175}Lu enriched to 99.8% and ^{176}Lu enriched to 71.6%, which were obtained from Oak Ridge National Laboratory. The oxide powder was finely dispersed in a solution of polystyrene in benzene. After evaporation of the benzene, the targets of approximately 10-

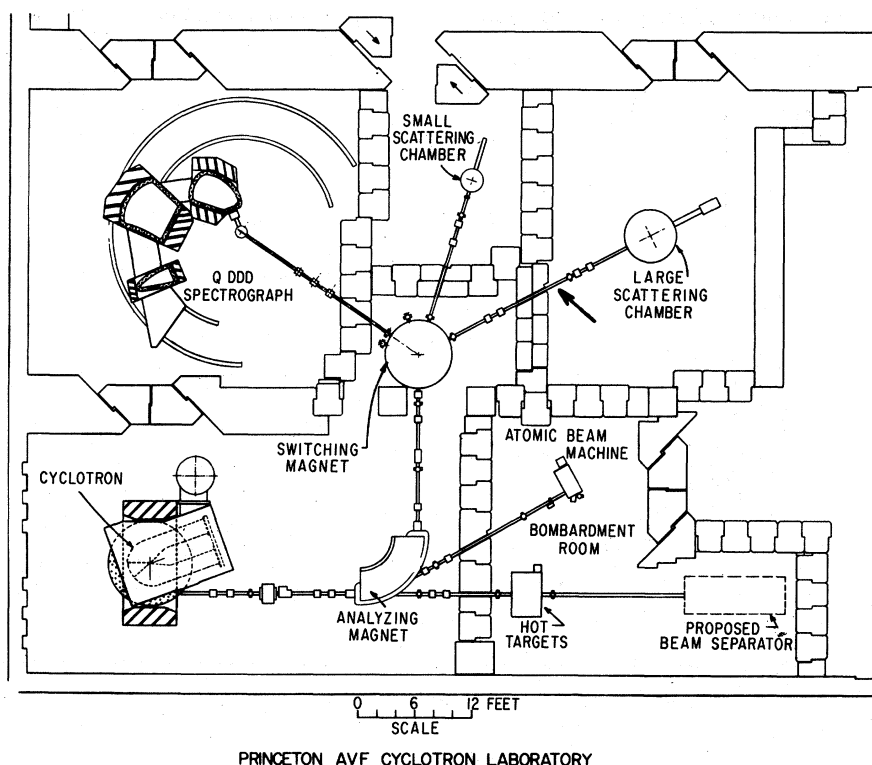


FIG. 2. Floor plan of the cyclotron experimental area. The small target chamber used for in-beam spectroscopy was located in the beam line at the position shown by the arrow.

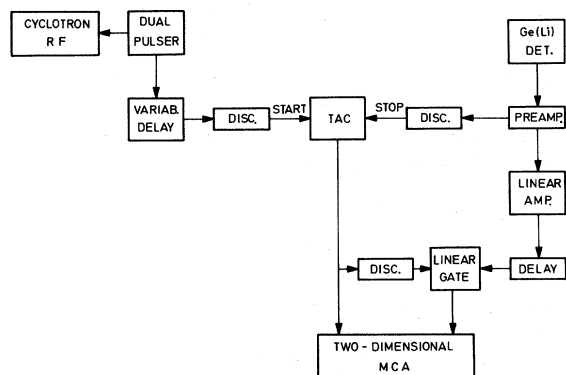


FIG. 3. Block diagram of the electronic system used to measure half-lives of isomeric states in the μsec range.

mg/cm^2 thickness could be mounted on target frames.

To facilitate the assignment of γ transitions to different tantalum isotopes, the energy of the α particles was varied between 24 and 48 MeV. At each α -particle energy, measurements with both the enriched ^{175}Lu and ^{176}Lu targets were obtained.

In order to perform the half-life measurements, the pulsed-beam technique was used. A block diagram of the main electronic components is shown in Fig. 3. The negative output of a dual pulsar is used to quench the rf supply of the cyclo-

tron, and the positive output is used to start a time-to-amplitude converter (TAC). The TAC was calibrated using signals from a pulsar which could be variably delayed from several nsec to 20 μsec .

The energy and time spectra are finally fed into an amplitude-to-digital converter of a two-dimensional 4096-channel analyzer. With this arrangement, half-lives as short as 1 μsec can be measured.

III. EXPERIMENTAL RESULTS

Some of the Ge(Li) γ -ray spectra obtained at a 90° angle to the beam following α -particle bombardment of the ^{175}Lu and ^{176}Lu targets are shown in Figs. 4-7. An evaluation of the γ -ray spectra obtained at different α energies with ^{175}Lu and ^{176}Lu targets confirms the results of SHR¹⁶ and Barnéoud *et al.*,¹⁷ who find a maximum in the cross section for the reaction $^{175}\text{Lu}(\alpha, 2n)^{177}\text{Ta}$ at an α energy of about 28 MeV. In order to study the properties and the decay of the 1355-keV high-spin isomeric state proposed by SHR,¹⁶ we have chosen an α energy of 30 MeV for the $^{175}\text{Lu}(\alpha, 2n)^{177m}\text{Ta}$ studies because of the slight spin dependence of the excitation function.¹⁹

Several measurements were carried out using pulsed α -particle beams from the cyclotron in the frequency range of 10-200 kHz. As an example, four consecutive γ -ray spectra obtained

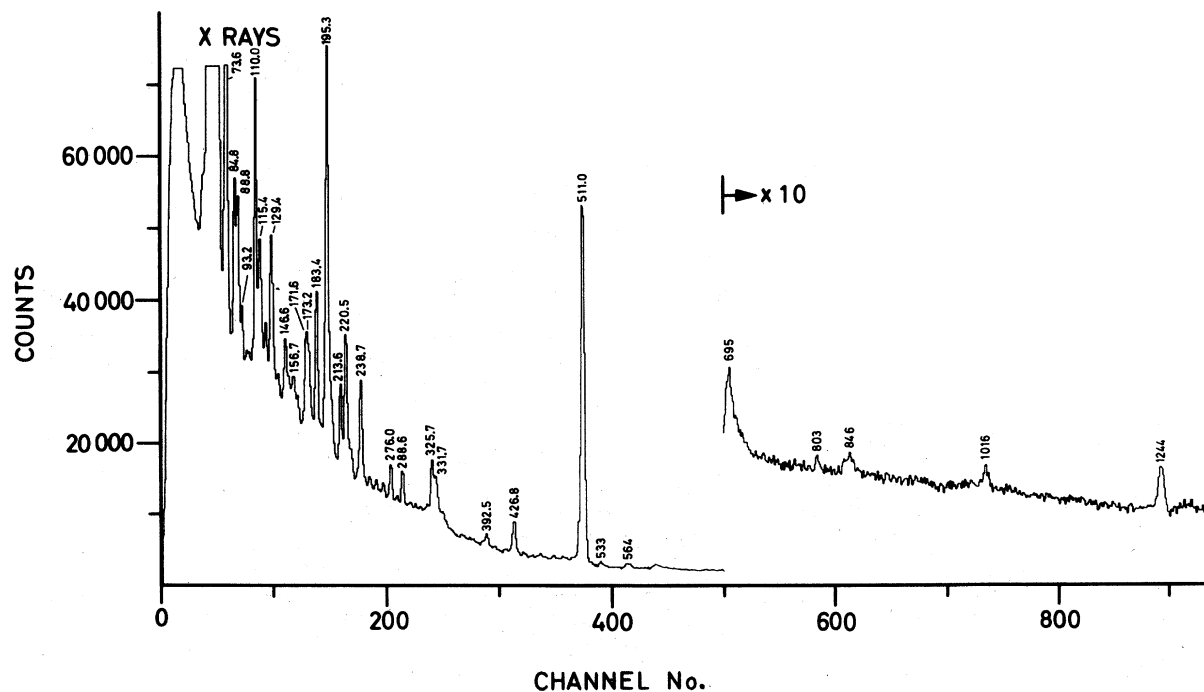


FIG. 4. In-beam γ -ray spectrum following the $^{176}\text{Lu}(\alpha, xn)$ reaction induced with 24-MeV α particles. This spectrum was obtained with a Ge(Li) detector at an angle of 90° with respect to the beam line.

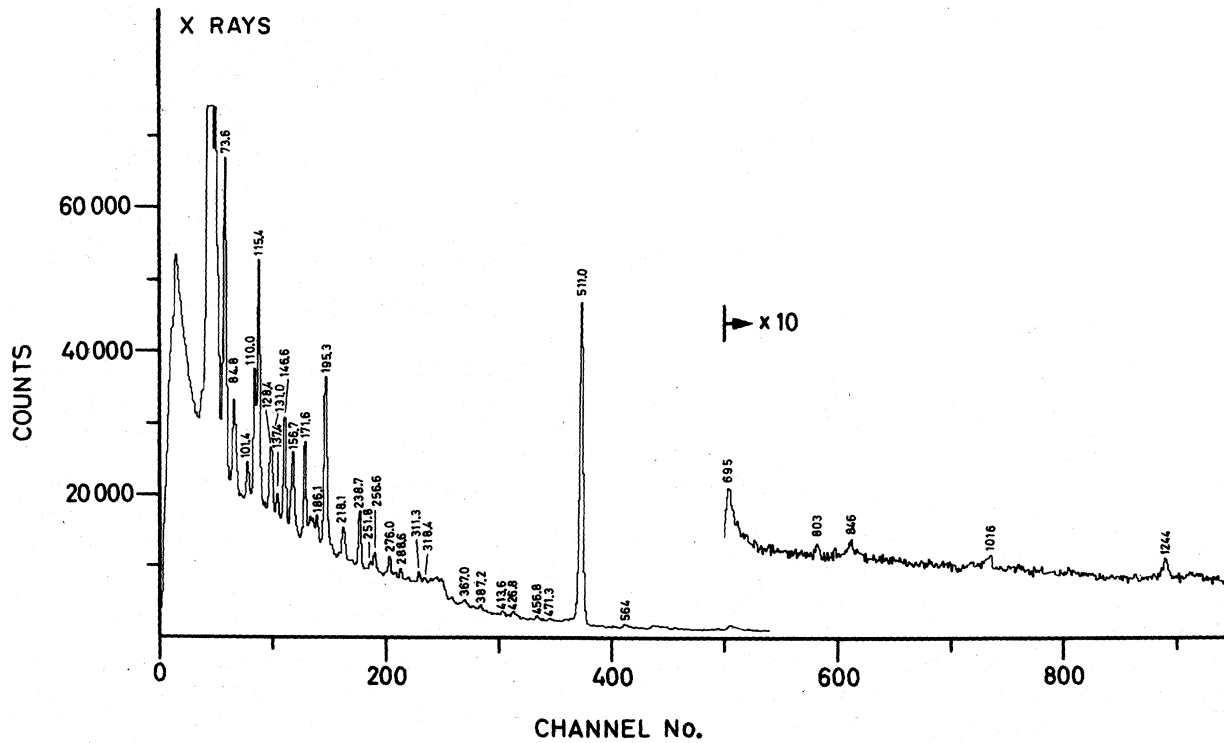


FIG. 5. In-beam γ -ray spectrum following the $^{175}\text{Lu}(\alpha, xn)$ reaction induced with 24-MeV α particles.

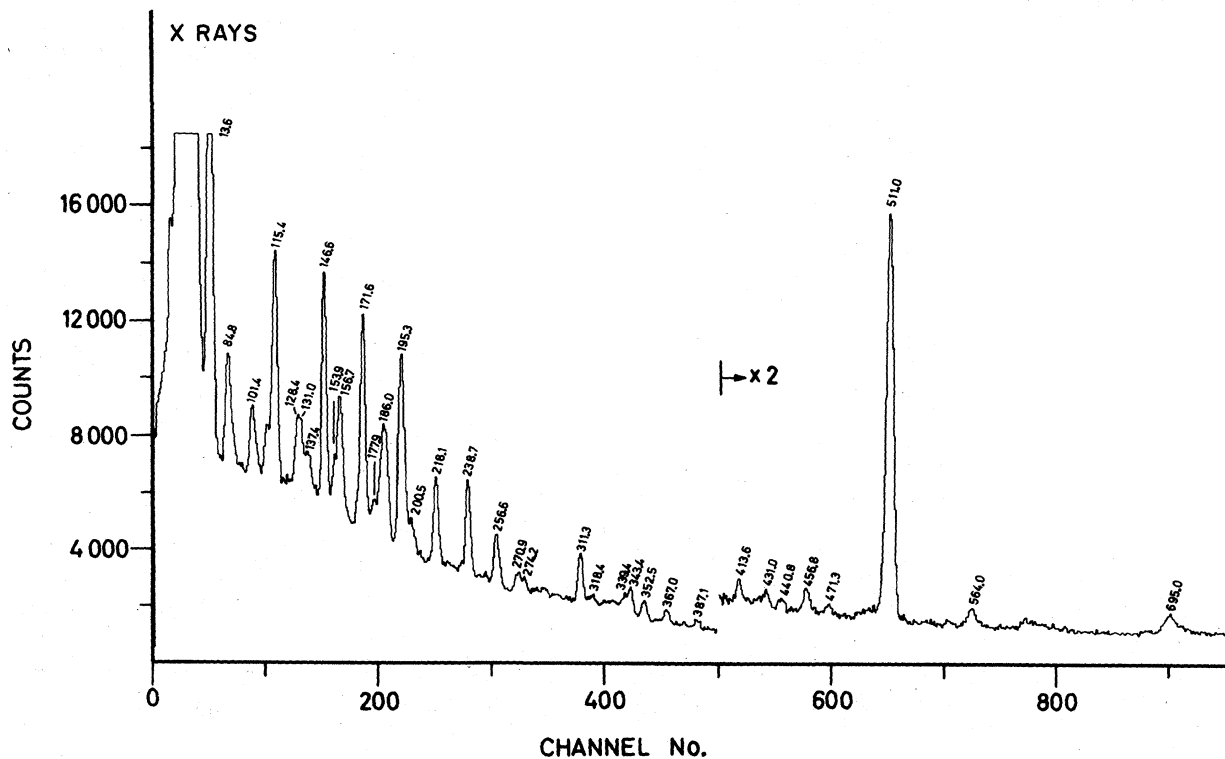


FIG. 6. In-beam γ -ray spectrum following the $^{175}\text{Lu}(\alpha, xn)$ reaction induced with 30-MeV α particles.

TABLE I. γ -ray energies and relative intensities of transitions assigned to the decay of the 1355-keV isomer in ^{177}Ta .

Energy (keV)	Relative γ intensity
146.6 \pm 0.2	58.0 \pm 7.0
171.6 \pm 0.2	79.2 \pm 9.0
195.3 \pm 0.3	80.3 \pm 10.0
218.1 \pm 0.3	60.8 \pm 7.0
238.7 \pm 0.3	68.7 \pm 8.0
311.3 \pm 0.4	100 ^a
318.3 \pm 0.4	11.6 \pm 1.6
367.0 \pm 0.4	23.4 \pm 2.5
413.5 \pm 0.5	22.0 \pm 2.5
456.8 \pm 0.5	36.5 \pm 3.5
550.0 \pm 0.8	15.2 \pm 4.0

^a Normalization.

between beam bursts of 30-MeV α particles on the ^{175}Lu target are shown in Figs. 8(a)–8(d). In this example each spectrum was measured for 5 μsec , so that a time range of 20 μsec was covered.

The strongest transitions observed in the spectra shown in Figs. 8(a)–8(d) are those assigned to the decay of the isomer at 1355 keV in ^{177}Ta (see Fig. 1). We have listed these transitions and their relative γ intensities in Table I. Although the spectra were measured at an angle of 90° with respect to the beam line, we believe that no angular-distrib-

ution effect has to be taken into account in the intensities, because an average waiting time of about 10 μsec was introduced after each beam burst. Since relaxation times are usually shorter, the spin alignment introduced by the nuclear reaction is probably completely destroyed during this waiting time.

The γ -ray energies agree very well with the results of the previous measurements by GGW,¹⁴ SHR,¹⁶ and Barnéoud *et al.*¹⁷ The relative γ -ray intensities cannot be compared with the previous results^{16, 17} obtained "in beam," because our values given in Table I have been measured between beam bursts of the cyclotron; they represent the results obtained in the decay of the isomeric state only.

The transitions listed in Table I all decay with the same half-life, an example of which is shown in Fig. 9. We obtain for the half-life of the isomeric state at 1355 keV

$$t_{1/2} = 5.02 \pm 0.20 \mu\text{sec}.$$

This value for the half-life is the weighted average of consistent results of several measurements covering the different time ranges of beam pulsing between 5 and 100 μsec . In order to provide a further check of our timing system, we also followed the decay (Fig. 10) of the 115-keV transition depopulating the $\frac{5}{2}^-$ isomeric state at 186 keV in ^{177}Ta (see Fig. 1). We obtain $t_{1/2}(186 \text{ keV}) = 3.6 \pm 0.2 \mu\text{sec}$, which is in good agreement with the

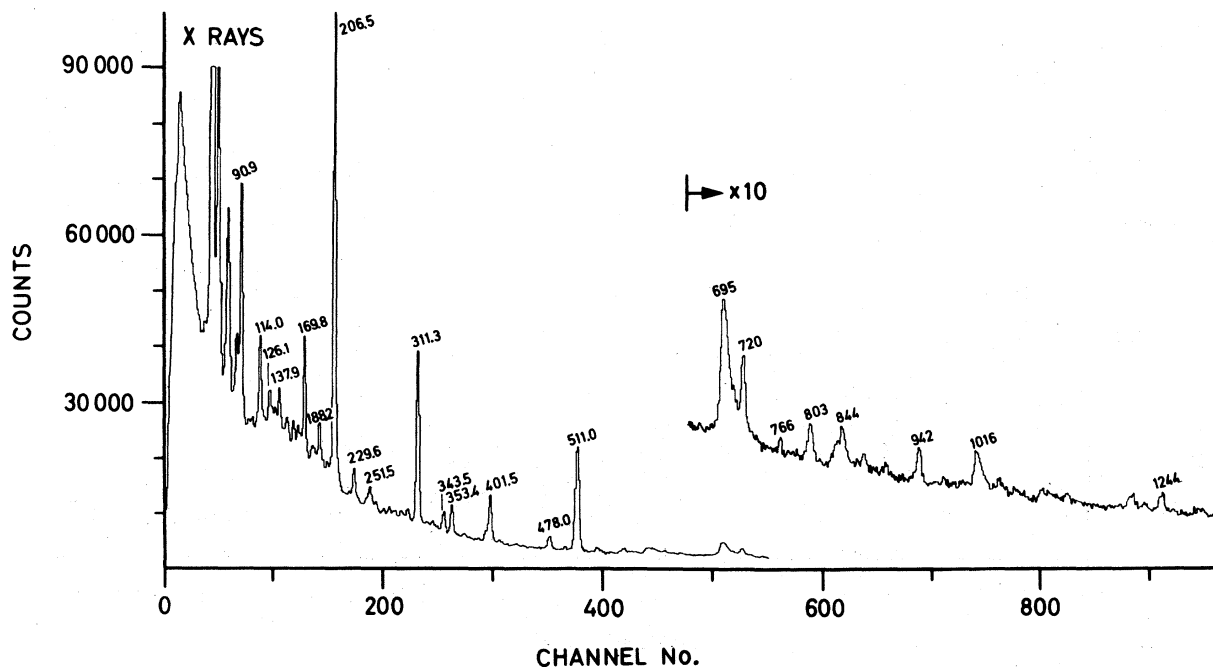


FIG. 7. In-beam γ -ray spectrum following the $^{175}\text{Lu}(\alpha, n)$ reaction induced with 48-MeV α particles.

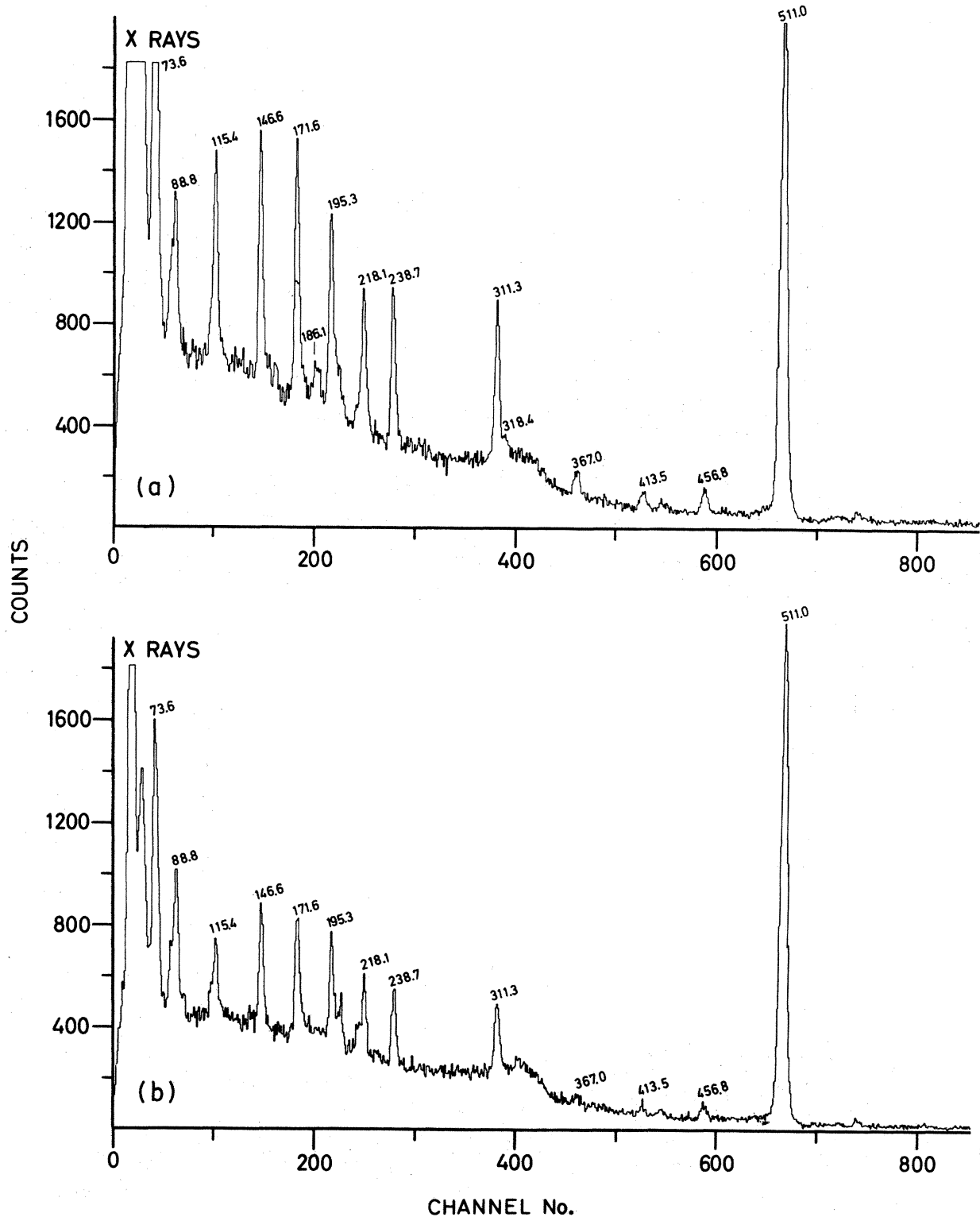


FIG. 8. Figure 8 consists of four parts: (a)–(d). Parts (c) and (d) appear on the following page. Four consecutive γ -ray spectra obtained at 5- μ sec intervals following the $^{175}\text{Lu}(\alpha, 2n)^{177}\text{Ta}$ reaction. These spectra were taken in the interval between beam bursts of 30-MeV α particles.

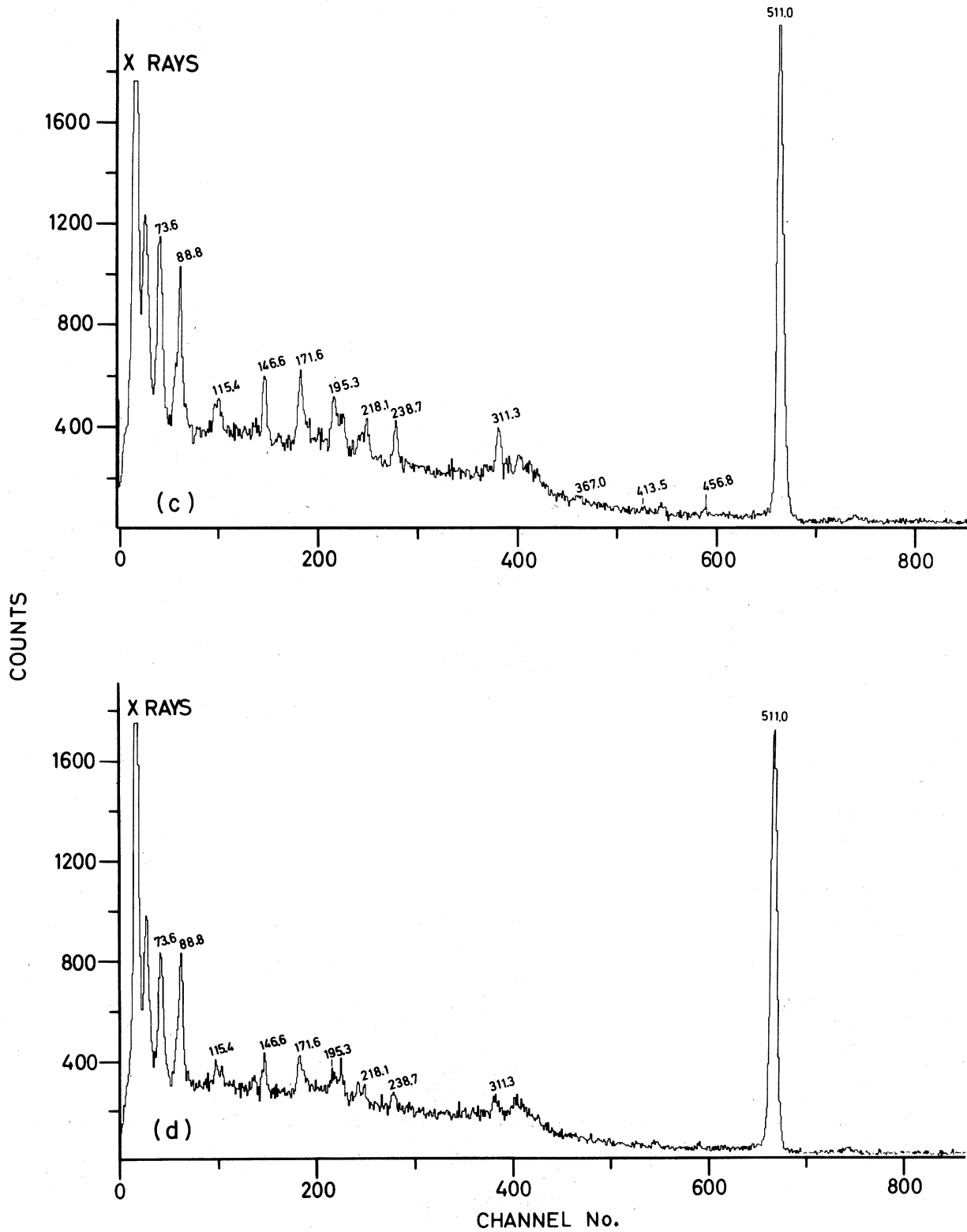


FIG. 8. (Continued). Parts (c) and (d).

previously known^{16, 20} value of 3.5 μsec .

In Fig. 8(d) a set of weak lines can be seen which have a longer half-life than those depopulating the 1355-keV isomeric state. In order to show that these transitions belong to a higher-mass tantalum isotope, we show in Fig. 11 for comparison the spectrum measured between beam bursts following the $^{176}\text{Lu}(\alpha, xn)$ reaction with 30-MeV α particles. Here we see in addition to the ^{177m}Ta transitions, the lines with energies 88.8, 93.2, 213.6, 325.7, 331.7, and 426.8 keV which are transitions in ^{178}Hf populated in the decay⁸ of 2.1-h ^{178}Ta , and a set of transitions with energies 173.2, 200.2, 227.3, 249.4, 392.5, and 474.8 keV. These transitions are those which become more prominent in the later spectra of Fig. 8. In Fig. 7, which shows the spectrum obtained in the $^{175}\text{Lu}(\alpha, xn)$ reaction with 48-MeV α particles, a set of lines with energies 90.9, 206.5, 311.3, 401.5, and 478.0 keV are found which have previously been assigned⁸ to ^{174}Hf and stem from the radioactive decay of ^{174}Ta to ^{174}Hf .

The $E2/M1$ mixing ratios for the cascade transitions within the $\frac{9}{2}[514]$ rotational band of ^{177}Ta (see Fig. 1) can be obtained from γ -ray intensity ratios between crossover $I \rightarrow I-2$ and cascade $I \rightarrow I-1$ transitions as explained below. With these the conversion coefficients and the total relative transition intensities can be calculated using the experimental γ -ray intensities. From the population and depopulation intensity balances of the $I = \frac{19}{2}$ and $\frac{17}{2}$ states of this band, the conversion coefficients of the 311- and 550-keV isomeric transitions can then be estimated as described below. The relative γ -ray intensities are given in Table I.

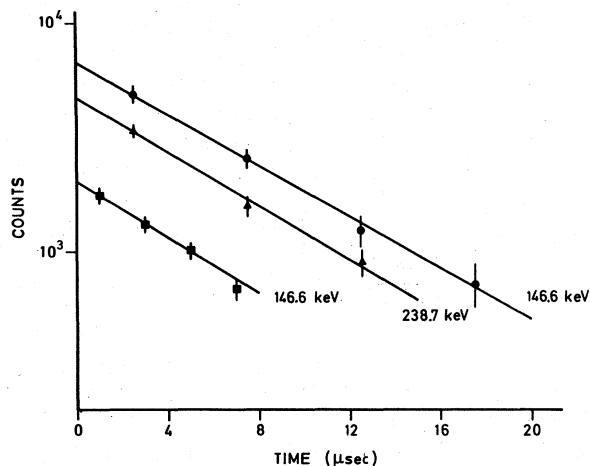


FIG. 9. Lifetime data for transitions following the decay of the 1355-keV isomer in ^{177}Ta . These data yield a half-life of $t_{1/2} = 5.02 \pm 0.20 \mu\text{sec}$. The two curves for the 146.6-keV transition are obtained from two different runs.

The theoretical conversion coefficients of the 238.7- and 456.8-keV transitions depopulating the $\frac{19}{2}^-$ level are $\alpha(239) = 0.38$ and $\alpha(457) = 0.025$, respectively. The total intensity depopulating the $\frac{19}{2}^-$ level is then $T_{\text{tot}}(\text{depop. } \frac{19}{2}) = 132$ (in relative units and with an uncertainty of approximately 15%). Using the value $T_{\gamma}(311) = 100$ (Table I) for the relative γ intensity of the 311-keV transition which populates this level, we obtain for the conversion coefficients $\alpha(311) = 0.32 \pm 0.15$. From a similar analysis SHR¹⁶ obtained $\alpha(311) = 0.37 \pm 0.18$. The theoretical conversion coefficients for $M1$, $M2$, $E2$, and $E3$ multiplicities are: $\alpha(311, M1) = 0.19$; $\alpha(311, M2) = 0.73$; $\alpha(311, E2) = 0.07$; and $\alpha(311, E3) = 0.31$. Thus our experimental value is compatible with a predominantly $M1$ or $E3$ character of the 311.3-keV transition. GGW¹⁴ have measured the K conversion coefficient of the 311.3-keV transition using an orange β spectrometer and found it to be of predominantly $M1$ multipolarity. A similar analysis can be carried out for the 550-keV isomeric transition. The result is compatible with an $E2$ multipole order for this transition, but the uncertainties are rather large.

IV. DISCUSSION

In the decay of the isomeric state at 1355 keV in ^{177}Ta which is shown in Fig. 1 only the $I = \frac{19}{2}$ and $\frac{17}{2}$ rotational states are populated, but no states with lower spins. Therefore, the spin of the isomer must be $I \geq \frac{19}{2}$. As was already pointed out by SHR,¹⁶ no single-particle orbital but quite a number of three-quasiparticle configurations consist-

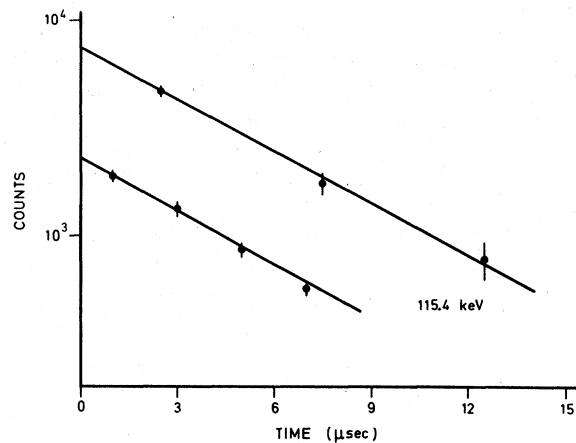


FIG. 10. Lifetime data for the 115-keV transition depopulating the $\frac{5}{2}^-$ state at 186 keV in ^{177}Ta . These data yield the value $t_{1/2} = 3.6 \pm 0.2 \mu\text{sec}$. The two curves are from two different runs.

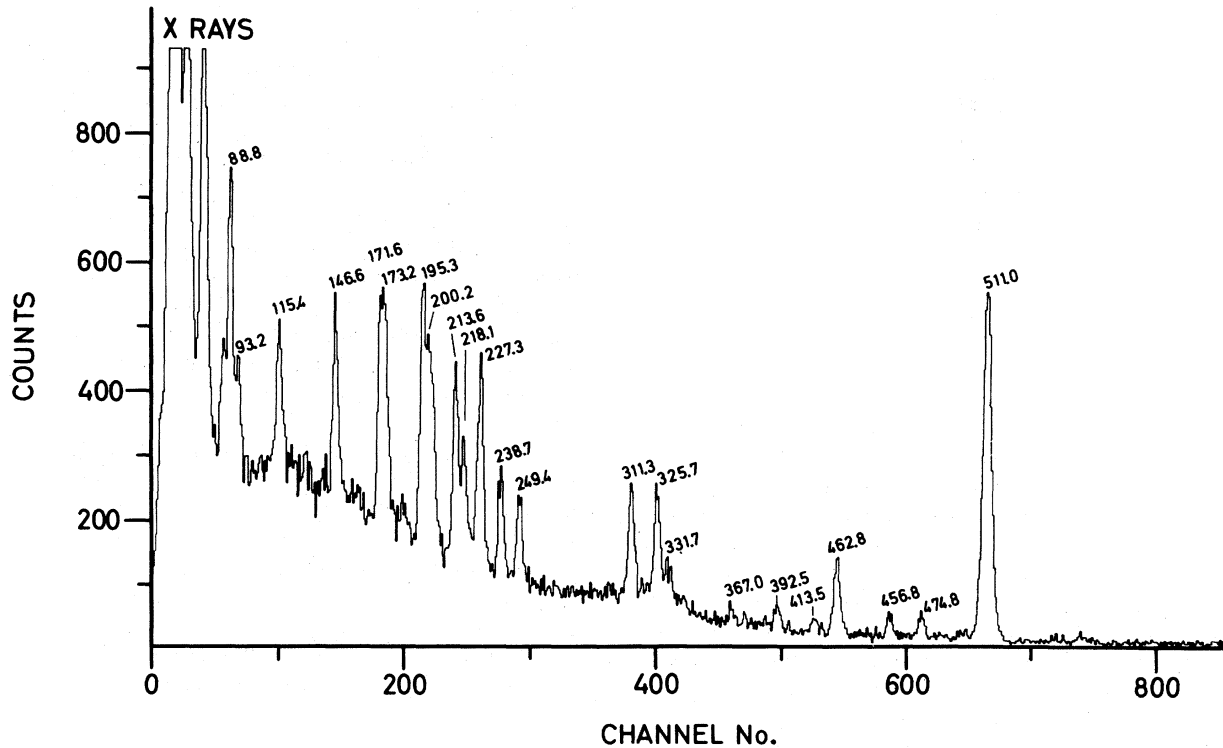


FIG. 11. γ -ray spectrum obtained between beam bursts following the $^{176}\text{Lu}(\alpha, n)$ reaction induced with 30-MeV α particles.

ing of a broken neutron or proton pair coupled to the odd proton of tantalum ($Z = 73$) can explain the intrinsic configuration of such a high-spin state. The measured lifetime of the isomer and the intensities of the depopulating transitions can be compared with transition rates usually found in the region of deformed nuclei. A convenient way to do this is to compare the partial lifetimes of the 311- and 550-keV transitions with the Weisskopf single-particle estimates.²¹ If one defines the degree of K forbiddenness⁹ as $k = \Delta K - L$ (with $L =$ multipole order of transition between states with K quantum numbers K_i and K_f , $\Delta K = |K_i - K_f|$)

one may write the retardation factor F in the form $F = f^k$, where f is the degree of forbiddenness per unit of k . Experimentally, values of f between 10 and 100 are found in this mass region.⁹ For a spin and parity assignment of $I^\pi = \frac{21}{2}^-$ to the 1355-keV isomeric state, the multiplicities of the 311- and 550-keV transitions are $M1$ and $E2$, respectively, and the degrees of K forbiddenness are $k = 5$ and 4 . In this case one finds the retardation factors $F(311 \text{ keV}) = 2 \times 10^{-7}$ and $F(550 \text{ keV}) = 8 \times 10^{-6}$ for the isomeric transitions. These values fall well within the range of experimentally observed retardation factors. For all other spin

TABLE II. Experimental ratios λ between crossover and cascade γ intensities, $E2/M1$ mixing ratios δ , and rotational-model parameters $(g_K - g_R)^2/Q_0^2$ for the $\frac{9}{2}[514]$ band in ^{177}Ta .

I_i	λ	δ		$(g_K - g_R)^2/Q_0^2$
		This work Branching	From Ref. 16 Ang. dist. Branching	
$\frac{11}{2}$	0.24 ± 0.11	...
$\frac{13}{2}$	0.146 ± 0.021	0.212 ± 0.015	0.23 ± 0.10	0.18 ± 0.02
$\frac{15}{2}$	0.291 ± 0.030	0.198 ± 0.010	0.25 ± 0.12	0.17 ± 0.02
$\frac{17}{2}$	0.362 ± 0.035	0.170 ± 0.008	0.25 ± 0.12	0.16 ± 0.02
$\frac{19}{2}$	0.532 ± 0.050	0.169 ± 0.008	0.21 ± 0.06	0.16 ± 0.02

and parity combinations considered for the isomer ($I^\pi = \frac{19}{2}^+, \frac{23}{2}^+, \frac{25}{2}^+$) no such agreement with the experimental retardations generally found for K -forbidden transitions in the region of deformed nuclei can be obtained. This fact, together with the evidence of $M1$ multipolarity for the 311-keV transition from the conversion coefficients, strongly supports the assignment of $I = \frac{21}{2}^-$ to the 1355-keV isomeric state.

The Nilsson configurations¹⁰ available in this region which can couple to a state with $I^\pi = \frac{21}{2}^-$ are:

$$\begin{aligned} & \left\{ \frac{7}{2}^+ [404]p, \frac{5}{2}^- [512]n, \frac{9}{2}^+ [524]n \right\} \frac{21}{2}^-; \\ & \left\{ \frac{9}{2}^- [514]p, \frac{5}{2}^- [512]n, \frac{7}{2}^- [514]n \right\} \frac{21}{2}^-; \\ & \left\{ \frac{5}{2}^+ [402]p, \frac{7}{2}^- [514]n, \frac{9}{2}^+ [624]n \right\} \frac{21}{2}^-; \\ & \left\{ \frac{5}{2}^+ [402]p, \frac{7}{2}^+ [404]p, \frac{9}{2}^- [514]p \right\} \frac{21}{2}^-. \end{aligned}$$

The couplings of a proton to a broken neutron pair seem to be somewhat favored because of their estimated energy, but a definite decision among these four configurations is not possible on the basis of the presently available data. Certainly the magnetic moment of the isomeric state and the properties of the rotational levels built on this state would be very helpful in the determination of its intrinsic configurations. Because of the small difference in energy expected for the configurations cited above, the actual makeup of the isomer may be a mixture of these.

In the decay of the 1355-keV isomeric state, the rotational band built on the $\frac{9}{2}^- [514]$ single-proton state at 73.6 keV is populated. SHR¹⁶ and Barnéoud *et al.*¹⁷ have shown that the rotational energy deviates only slightly from a two-parameter energy expression.

The transition probabilities provide a further test of the predictions of the rotational model. For an unperturbed band the $E2/M1$ mixing ratios $\delta^2 = T_\gamma(E2)/T_\gamma(M1)$ can be derived from the ratios between crossover $I \rightarrow I-2$ and cascade $I \rightarrow I-1$ γ intensities:

$$\lambda = \frac{T_\gamma(E2, \Delta I = 2)}{T_\gamma(E2, \Delta I = 1)} \frac{\delta^2}{(1 + \delta^2)}. \quad (\text{I})$$

The mixing ratios are then related to the gyromagnetic factors for the particle and collective motion, g_K and g_R , respectively, and to the in-

trinsic quadrupole moment Q_0 by (for $K \neq \frac{1}{2}$; E_γ in keV, Q_0 in 10^{-24} cm²)

$$\frac{1}{\delta^2} = \frac{2.87 \times 10^5 (2I+2)(2I-2)}{E_\gamma^2} \frac{(g_K - g_R)^2}{Q_0^2}. \quad (\text{II})$$

In Table II we have listed the crossover/cascade intensity ratios λ , the mixing parameters δ , and the rotational-model expressions $(g_K - g_R)^2/Q_0^2$. Our results for the mixing parameters are in agreement with those obtained by SHR¹⁶ from angular-distribution and branching-ratio measurements, which are also given in the table.

The results for $(g_K - g_R)^2/Q_0^2$ show an increase of about 30%, in contradiction to the predictions of the adiabatic rotational model which assumes g_K , g_R , and Q_0 to be independent of the spin I within a rotational band. The deviation of the experimental values from the predicted constancy within the $\frac{9}{2}^- [514]$ rotational band is an indication of non-adiabatic effects. In this case, however, it is no longer permissible to apply formulas (I) and (II) to derive the mixing ratios δ^2 and $(g_K - g_R)^2/Q_0^2$. The deviation from the simple rotational-model prediction found here is larger than in other rotational bands studied up to high-spin values.^{12, 22-27} To obtain an estimate for the gyromagnetic factor g_R , however, we have simply taken the average for $(g_K - g_R)^2/Q_0^2 = 0.017$ and multiplied by a value of $Q_0 = 7.2$ b for the quadrupole moment²⁷ taken from the neighboring ^{177}Hf , thus obtaining $(g_K - g_R) = 0.94$. The sign of $(g_K - g_R)$ is equal to the sign of the $E2/M1$ mixing parameter, which was found to be positive by SHR.¹⁶ Using Nilsson wave functions¹⁰ and an effective spin g factor of $g_S^{\text{eff}} = 0.6 g_S^{\text{free}}$ we obtain $g_K = 1.24$ for the $\frac{9}{2}^- [514]$ band. Using this value for g_K and our experimental average value for $(g_K - g_R)$, $g_R = 0.30$ may be deduced for the gyromagnetic factor of the collective motion. This value is in agreement with results of the cranking-model calculations of Prior, Boehm, and Nilsson.²⁸

ACKNOWLEDGMENT

The authors wish to thank Dr. R. E. Pollock and the staff of the Princeton Cyclotron for their assistance in operating the accelerator. The help of F. W. Loeser, Jr., and R. Nuttall during the experiment is greatly appreciated.

†Work supported by the U. S. Atomic Energy Commission.

*Present address: Institut für Strahlen- und Kernphysik, Universität Bonn, West Germany.

¹H. Morinaga and P. C. Gugelot, Nucl. Phys. **46**, 210 (1963).

²J. O. Newton, F. S. Stephens, R. M. Diamond, W. H. Kelly, and D. Ward, Nucl. Phys. **A141**, 631 (1970).

³J. Borggreen, N. J. S. Hansen, J. Pedersen, L. Westgaard, J. Zylicz, and S. Bjørnholm, Nucl. Phys. **A96**, 561 (1967).

⁴S. A. Hjorth, H. Ryde, and B. Skånberg, Arkiv Fysik

- 38, 537 (1968).
⁵H. Hübel, R. A. Naumann, and P. K. Hopke, Phys. Rev. C **2**, 1447 (1970).
⁶T. W. Conlon, Nucl. Phys. **A136**, 70 (1969).
⁷T. Yamazaki, Phys. Rev. C **1**, 290 (1970).
⁸C. M. Lederer, J. M. Hollander, and I. Perlman, *Table of Isotopes* (Wiley, New York, 1967), 6th ed.
⁹O. Nathan and S. G. Nilsson, in *Alpha-, Beta-, and Gamma-Ray Spectroscopy*, edited by K. Siegbahn (North-Holland, Amsterdam, 1965), Chap. X.
¹⁰S. G. Nilsson, Kgl. Danske Videnskab. Selskab, Mat.-Fys. Medd. **29**, No. 16 (1955).
¹¹R. G. Helmer and C. W. Reich, Nucl. Phys. **A114**, 649 (1968).
¹²H. Hübel, R. A. Naumann, M. L. Andersen, J. S. Larsen, O. B. Nielsen, and N. O. Roy Poulsen, Phys. Rev. C **1**, 1845 (1970).
¹³B. Skånberg, H. Ryde, and S. A. Hjorth, Research Institute for Physics, Stockholm, Annual Report 1968 (unpublished), p. 29; Research Institute for Physics, Stockholm, Annual Report 1969 (unpublished), p. 33; C. Foin, Th. Lindblad, B. Skånberg, H. Ryde, and J. Valentin, Research Institute of Physics, Stockholm, Annual Report 1970 (unpublished), p. 61.
¹⁴J. S. Geiger, R. L. Graham, and D. Ward, AECL Report No. AECL 3257, 1968 (unpublished), p. 28.
¹⁵L. A. Beach, C. R. Gossett, R. C. Carlson, G. T. Emery, L. R. Mesker, W. T. Sloan, and P. P. Singh, Bull. Am. Phys. Soc. **647** (1970); P. P. Singh, L. R. Mesker, G. T. Emery, C. R. Gossett, and L. A. Beach, *ibid.* **16**, 514 (1971).
¹⁶B. Skånberg, S. A. Hjorth, and H. Ryde, Nucl. Phys. **A154**, 641 (1970).
¹⁷D. Barnéoud, C. Foin, A. Baudry, A. Gizon, and J. Valentin, Nucl. Phys. **A154**, 653 (1970).
¹⁸Princeton University Nuclear Physics Progress Report No. PUC-937-359, 1969 (unpublished); and No. PUC-937-378, 1970 (unpublished).
¹⁹J. O. Newton, Nucl. Phys. **A108**, 353 (1968).
²⁰B. Ader, Ph.D. thesis, University of Paris, 1969 (unpublished).
²¹A. H. Wapstra, G. J. Nijgh, and R. van Lieshout, *Nuclear Spectroscopy Tables* (North-Holland, Amsterdam, 1959).
²²J. de Boer and J. D. Rogers, Phys. Letters **3**, 304 (1963).
²³D. Ashery and G. Goldring, Z. Naturforsch. **21a**, 936 (1966).
²⁴F. Boehm, G. Goldring, G. B. Hagemann, G. D. Symons, and A. Toeter, Phys. Letters **22**, 627 (1966).
²⁵G. G. Seaman, E. M. Bernstein, and J. M. Palms, Phys. Rev. **161**, 1223 (1967).
²⁶A. J. Haverfield, F. M. Bernthal, and J. M. Hollander, Nucl. Phys. **A94**, 337 (1967).
²⁷H. Hübel, C. Günther, K. Krien, H. Toschinski, K.-H. Speidel, B. Klemme, G. Kumbartzki, L. Gidefeldt, and E. Bodenstedt, Nucl. Phys. **A127**, 609 (1969).
²⁸O. Prior, F. Boehm, and S. G. Nilsson, Nucl. Phys. **A110**, 257 (1968).

Fission-Fragment Angular Momentum in Charged-Particle-Induced Fission.

I. ¹³⁴Cs and ¹¹⁵Cd Isomer Ratios*

W. D. Loveland and Y. S. Shum

Oregon State University, Corvallis, Oregon 97311

(Received 16 August 1971)

The ¹³⁴Cs and ¹¹⁵Cd isomer ratios have been measured for the following cases of charged-particle-induced fission: ²³⁸U(35-MeV α, f), ²³²Th(20-MeV d, f), ²²⁶Ra(19-MeV d, f), and ²⁰⁹Bi(35-MeV α, f). The values of the ¹³⁴Cs isomer ratio were 0.52 ± 0.02 , 0.64 ± 0.01 , and 0.20 ± 0.05 for the fission of ²³⁸U, ²³²Th, and ²²⁶Ra, respectively. The ¹¹⁵Cd isomer ratios were 0.090 ± 0.006 , 0.059 ± 0.007 , 0.90 ± 0.12 , and 0.9 ± 0.2 for the fission of ²³⁸U, ²³²Th, ²²⁶Ra, and ²⁰⁹Bi, respectively. The low values of the ¹¹⁵Cd isomer ratios for the fission of ²³⁸U and ²³²Th are attributed to decay-scheme effects. The average initial fragment angular momentum was deduced from the isomer-ratio values using the Vandenbosch-Huizenga formalism. The values obtained were $(11 \pm 1)\hbar$, $(13 \pm 1)\hbar$, and $(7 \pm 2)\hbar$ for the ¹³⁴Cs fragment in the fission of ²³⁸U, ²³²Th, and ²²⁶Ra, respectively. Values of $>(15 \pm 4)\hbar$ and $>(13 \pm 4)\hbar$ for the ¹¹⁵Cd fragment in the fission of ²²⁶Ra and ²⁰⁹Bi were obtained. These results are discussed in terms of current theories about the origin of the fragment angular momentum in fission.

I. INTRODUCTION

One of the most studied and least understood aspects of the fission process is the scission point. This is the point in the fission process where the deformed, elongated nucleus "necks in" and actual-

ly divides into the fragments. A knowledge of the dynamics of the nascent fragment motion at this point would appear to be important, especially in view of recent theoretical attempts¹ to describe fission by "working backwards" in time from the scission point. In addition, two studies^{2,3} of the